JACS
JOURNAL OF THE AMERICAN CHEMICAL SOCIETY

COMMUNICATION

pubs.acs.org/JACS

DNA Electron Injection Interlayers for Polymer Light-Emitting Diodes

Peter Zalar,[†] Daniel Kamkar,[†] Rajesh Naik,[‡] Fahima Ouchen,[‡] James G. Grote,[‡] Guillermo C. Bazan,*[,†] and Thuc-Quyen Nguyen*[,†]

[†]Center for Polymers and Organic Solids, Department of Physics, and Department of Chemistry & Biochemistry, University of California, Santa Barbara, California 93106, United States

[‡]Materials and Manufacturing Directorate, Air Force Research Laboratory, Wright-Patterson AFB, Ohio 45433, United States

Supporting Information

ABSTRACT: Introduction of a DNA interlayer adjacent to an Al cathode in a polymer light-emitting diode leads to lower turn-on voltages, higher luminance efficiencies, and characteristics comparable to those observed using a Ba electrode. The DNA serves to improve electron injection and also functions as a hole-blocking layer. The temporal characteristics of the devices are consistent with an interfacial dipole layer adjacent to the electrode being responsible for the reduction of the electron injection barrier.

Interfacial effects often dominate the performance of optoelectronic devices based on organic semiconducting materials.[1] A relevant example concerns the energetic barriers to charge injection and extraction at electrode−organic interfaces. In the case of polymer light-emitting diodes (PLEDs),[2] such barriers can lead to unbalanced electron and hole densities and therefore lower device efficiencies.[3] Electron injection barriers arise because the lowest unoccupied molecular orbital (LUMO) energy levels of typical electroluminescent semiconducting conjugated polymers are not well matched with the work functions of stable metal cathodes such as Al, Au, and Ag. Low-work-function metals such as Ca and Ba can be used to circumvent this problem at the expense of device stability because of their more pronounced sensitivity toward air.[4]

Several approaches for reducing charge injection barriers in PLEDs and other organic devices have been reported.[5,6] For example, multilayer architectures can be designed that incorporate an electron injection/transport layer adjacent to the cathode. One class of materials that has found use in this respect involves conjugated polyelectrolytes (CPEs)[7] and oligoelectrolytes,[8] which are structurally defined by an electronically delocalized backbone with pendant groups bearing ionic functionalities. While there is a range of possible interfacial phenomena that can modify the contacts,[1a] two mechanisms have dominated the discussion of CPE function. The first is usually observed with thick layers and involves initial ion migration upon application of an external bias, which leads to a redistribution of the electric field within the device and a longer response time.[6b,c] A steep electric field gradient is generated close to the electrode as a result of this ion motion, which aids electron injection into the LUMO of the underlying polymer.[9] The second mechanism involves the presence of an interfacial dipole layer that modifies the effective work function of the cathode.[1c,10,11a] These conditions lead to faster device turn-on times and direct electron injection into the electroluminescent layer.

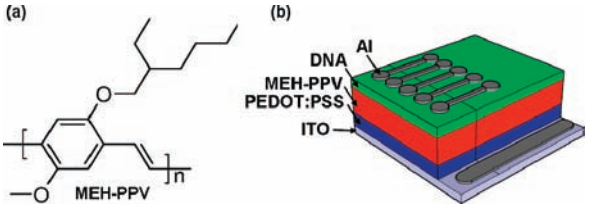

Figure 1. (a) Molecular structure of MEH-PPV. (b) PLED test structure incorporating a DNA interlayer between the Al cathode and the electroluminescent MEH-PPV layer.

It occurred to us that an interfacial dipole layer could be achieved atop the electroluminescent layer of a PLED with a standard polyelectrolyte (i.e., one that does not contain a conjugated backbone).[12] Furthermore, it seemed challenging to focus on naturally occurring renewable materials. As described here, we show that DNA can serve as a useful interlayer to improve the performance of organic electronic devices. Previous uses of DNA in organic electronics include integration as a 500 nm thick dielectric in organic field-effect transistors and as a hole-transporting/electron-blocking layer in organic LEDs when a layer (∼20 nm thick) is introduced near the anode.[13]

The DNA examined in this study was purified by the Chitose Institute of Science and Technology from waste products of the salmon fishing industry via an enzyme isolation process.[13] The molecular weight of the DNA was typically >8000 kDa as determined by gel-phase electrophoresis.[13] The PLED device test structures used in these studies involved platforms in which poly[2-methoxy-5-(2′-ethylhexyloxy)-*p*-phenylenevinylene] (MEH-PPV) was deposited atop poly(3,4-ethylenedioxythiophene):poly(styrenesulfonate) (PEDOT:PSS)-treated ITO substrates, as shown in Figure 1.[6c] The DNA was spin-coated from a highly polar solvent in order to minimize disturbance of the underlying charge-neutral layer.[14] Evaporation of the cathode constituted the final fabrication step, yielding a device with an area of 4.5 mm^2. Cathodes composed of Al or Ba were employed in order to illustrate the effect of using metals with different work functions. In the following study, only an Al electrode was used in conjunction with the DNA interlayer.

Considerable attention was dedicated to the DNA deposition method. The best devices were obtained by dissolving the DNA

Received: March 1, 2011
Published: June 09, 2011

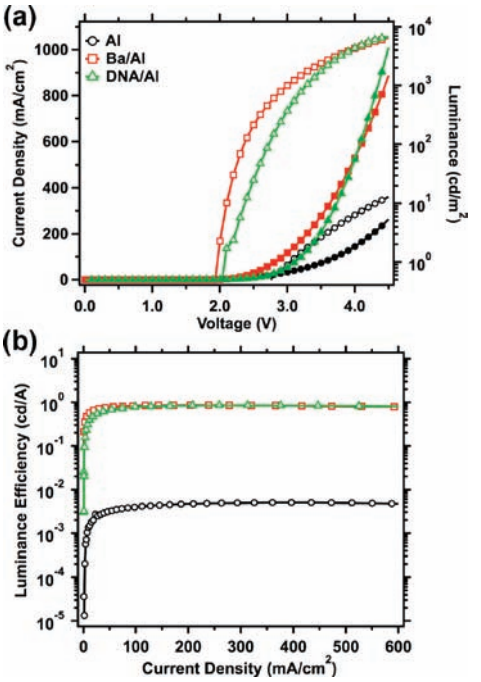

Figure 2. (a) $J-V$ (closed symbols) and $L-V$ (open symbols) plots and (b) luminance efficiency characteristics of PLEDs with the following device structures: ITO/PEDOT:PSS/MEH-PPV/Ba/Al (red squares), ITO/PEDOT:PSS/MEH-PPV/DNA/Al (green triangles), and ITO/PEDOT:PSS/MEH-PPV/Al (black circles).

in a 90:10 (v/v) methanol/water solvent mixture. The DNA solution was first filtered through a poly(vinylidene fluoride) filter with a pore size of 0.45 μm and then spin-coated at 1500 rpm for 60 s atop the MEH-PPV film. Figure 2a shows typical plots of current density (J) and luminance (L) versus applied voltage for devices with DNA/Al cathodes together with the characteristics observed for control devices with Ba and Al cathodes. In all cases, the electroluminescence maximum was characteristic of MEH-PPV, with a maximum centered at 560 nm. The most significant comparison can be drawn between the DNA/Al and Al devices, where the former required a considerably reduced applied bias to achieve $L = 10$ cd/m^2 (2.3 ± 0.1 V for DNA/Al vs 4.1 ± 0.3 V for Al) and gave significantly higher L values at 4.5 V (5700 ± 620 cd/m^2 for DNA/Al vs 25.5 ± 10.5 cd/m^2 for Al). Indeed, the DNA/Al device showed characteristics in both J and L that resemble those of the Ba device, for which a close to ohmic contact existed between the cathode and the MEH-PPV layer. All of these features led to similar luminance efficiencies (Figure 2b) for the DNA/Al and Ba devices (0.80 ± 0.15 and 0.86 ± 0.15 cd/A, respectively) that were much higher than that of the Al-only counterpart [$(6.5 \pm 2.3) \times 10^{-3}$ cd/A]. We note that the errors in the measurements above correspond to one standard deviation for measurements on 10 independently fabricated devices. The collected set of experiments therefore demonstrates that insertion of the DNA interlayer drastically improves the device efficiency. Furthermore, since the hole injection interface is unaffected by the DNA, we surmise that the higher J values observed in Figure 2a for the MEH-PPV/DNA/Al device relative to those for MEH-PPV/Al are due to improved electron injection at the cathode.[15]

The response times of the DNA/Al and Al devices were examined to gain insight into the mechanism by which DNA

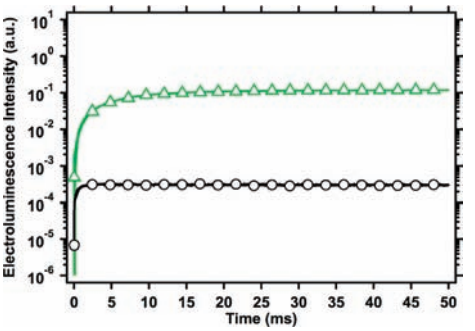

Figure 3. Plots of EL intensity vs time for MEH-PPV/Al (black ○) and MEH-PPV/DNA/Al (green △) devices.

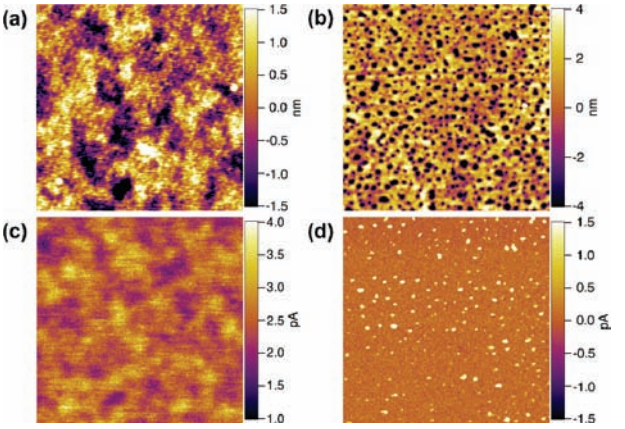

Figure 4. (a, b) Morphology and (c, d) current measurements of (a, c) MEH-PPV and (b, d) MEH-PPV/DNA surfaces. The voltage in the current measurements was +2 V DC for (c) and +5 V for (d). The rms roughness was 0.8 nm in (a) and 2.8 nm in (b). The size of the images is 2 μm × 2 μm.

incorporation improves the electron injection. These measurements involved applying a rectangular voltage pulse at 3.5 V, as described previously.[8a] The electroluminescence (EL) signal was detected using a Si photodiode coupled with an oscilloscope, and the results are shown in Figure 3. The time response of the MEH-PPV/Al device (defined as the time required to reach 50% of the maximum luminance) was <1 ms, whereas 14 ms was observed for the MEH-PPV/DNA/Al device. We also note that the final ratio of the intensities of the EL response in Figure 3 after ~30 ms correlates with the luminance ratio in the steady-state measurement in Figure 2. The response time of the MEH-PPV/DNA/Al device suggests that the screening of the electrical field due to ion motion within the DNA interlayer plays a minor role in increasing the current density shown by the black and green curves in Figure 2a.[11b] For comparison, thick CPE electron transport layers can yield multisecond response times.[6b] Therefore, we conclude from these data that the improved electron injection after DNA deposition is more reasonably attributed to the formation of a suitably aligned dipole adjacent to the Al electrode.[11c]

To further understand the effect of the DNA interlayer on the device function, the surface properties were probed by scanning probe techniques. Figure 4a,b displays topographic images of ITO/PEDOT:PSS/MEH-PPV/Al and ITO/PEDOT:PSS/MEH-PPV/DNA/Al devices scanned between the Al electrodes, as determined by atomic force microscopy (AFM). The MEH-PPV surface was a smooth film (rms roughness = 0.8 nm), while the

MEH-PPV/DNA films showed a weblike morphology (presumably DNA) with pinholes on the order of 12−16 nm deep (rms roughness = 2.8 nm). These data indicate an average DNA thickness of 15 ± 3 nm. The overall morphology in Figure 4b is consistent with poor wetting between the hydrophobic MEH-PPV and the polyelectrolyte. Additionally, there were no changes in the morphology after exposure to moist air,[16] even after 14 h (see the Supporting Information). We also note that spin-coating of the DNA from other solvent mixtures led to other irregular morphologies (see the Supporting Information).

Figure 4c,d shows conductive AFM images, which were used to gain insight into the nanoscale conduction characteristics across the MEH-PPV and MEH-PPV/DNA layers. By using a gold-coated AFM tip, one obtains little to no barrier for hole injection because of the match between the work function of gold and the highest occupied molecular orbital (HOMO) energy of MEH-PPV. This feature allows one to collect hole current through the MEH-PPV layer.[17] At an applied DC bias of 2 V, an average current of ∼2.5 pA was observed across the MEH-PPV surface (Figure 4b). After DNA was spin-coated atop the MEH-PPV layer, little current was observed at an applied bias of 2 V across the entire film. When the bias was increased to 5 V, an average current of ∼0.1 pA was observed (Figure 4d), which is attributed to an increase in current from the sites corresponding to the pinhole regions shown in Figure 4b. These data indicate that DNA (a) exists over the entire surface of the semiconducting film, including a thin layer within the pinhole regions, and (b) acts as an effective hole-blocking layer. The improved function of the devices in Figure 2 upon introduction of the DNA therefore arises from the combination of improved electron injection and blocking of holes, ultimately leading to balanced charge carriers.[18]

To summarize, a naturally occurring and readily available polyelectrolyte, namely, DNA, was used to significantly improve PLED efficiencies utilizing MEH-PPV electroluminescent layers. Introduction of the DNA interlayer beneath the Al cathode led to an increase in efficiency from $(6.5 \pm 2.3) \times 10^{-3}$ to 0.80 ± 0.15 cd/A. Comparison of the of the $J-V$ characteristics of the MEH-PPV/DNA/Al and MEH-PPV/Al devices showed that the DNA layer facilitates electron injection. The temporal response of the MEH-PPV/DNA/Al device shown in Figure 3 can be accommodated more easily within a mechanistic framework where ion motion plays only a minor role in modifying the electron injection barriers. We therefore propose that a dipole layer that modifies the effective work function of Al is formed. AFM experiments showed that the deposition of DNA under the conditions described here led not to a homogeneous film but instead to a weblike morphology. Such features are anticipated under circumstances where there is poor wetting with the hydrophobic underlayer. Conductive AFM scans showed that DNA also serves as a hole-blocking layer; with current observed only within the areas corresponding to the "pinholes" at high applied voltages. Since a thick DNA layer is anticipated to be insulating toward both electrons and holes, we propose that the electrons are most reasonably injected into the MEH-PPV within the thinnest portions of the interlayer.

■ ASSOCIATED CONTENT

Supporting Information. Experimental details and additional AFM images. This material is available free of charge via the Internet at http://pubs.acs.org.

■ AUTHOR INFORMATION

Corresponding Author
bazan@chem.ucsb.edu; quyen@chem.ucsb.edu

■ ACKNOWLEDGMENT

This work was funded by an Air Force Research Laboratory Seed Grant (AFOSR/FA9550-08-1-0248) and a Camille Dreyfus Teacher-Scholar Award. P.Z. was supported by the Department of Energy Office of Basic Energy Sciences (DE-SC0002368). D.K. was supported by an NSF CAREER Award (DMR 0547639). T.-Q.N. is an Alfred P. Sloan Foundation Research Fellow. The authors thank Aidee Duarte for help in the processing of DNA thin films.

■ REFERENCES

(1) (a) Ishii, H.; Sugiyama, K.; Ito, E.; Seki, K. *Adv. Mater.* **1999**, *11*, 605–625. (b) Kahn, A.; Koch, N.; Gao, W.-Y. *J. Polym. Sci., Part B: Polym. Phys.* **2003**, *41*, 2529–2548. (c) Wu, H.-B.; Huang, F.; Peng, J.-B.; Cao, Y. *Org. Electron.* **2005**, *6*, 118–128.

(2) Burroughes, J. H.; Bradley, D. C. C.; Brown, A. R.; Marks, R. N.; Mackay, K.; Friend, R. H.; Burns, P. L.; Holmes, A. B. *Nature* **1990**, *347*, 539–541.

(3) Friend, R. H.; Gymer, R. W.; Holmes, A. B.; Burroughes, J. H.; Marks, R. N.; Taliani, C.; Bradley, D. C. C.; Dos Santos, D. A.; Brédas, J.-L.; Lögdlund, M.; Salaneck, W. R. *Nature* **1999**, *397*, 121–128.

(4) (a) Bröms, P.; Birgersson, J.; Johansson, N.; Lögdlund, M.; Salaneck, W. R. *Synth. Met.* **1995**, *74*, 179–181. (b) Carter, J. C.; Grizzi, I.; Heeks, S. K.; Lacey, D. J.; Latham, S. G.; May, P. G.; Ruiz de los Paños, O.; Pichler, K.; Towns, C. R.; Wittmann, H. F. *Appl. Phys. Lett.* **1997**, *71*, 34–36.

(5) (a) Burgi, L.; Richards, T. J.; Friend, R. H.; Sirringhaus, H. *J. Appl. Phys.* **2003**, *94*, 6129–6137. (b) Pesavento, P. V.; Puntambekar, K. P.; Frisbie, C. D.; McKeen, J. C.; Ruden, P. P. *J. Appl. Phys.* **2006**, *99*, No. 094504. (c) Gong, X.; Wang, S.; Moses, D.; Bazan, G. C.; Heeger, A. J. *Adv. Mater.* **2005**, *17*, 2053–2058.

(6) (a) Wu, H.-B.; Huang, F.; Mo, Y.-Q.; Yang, W.; Wang, D.-L.; Peng, J.-B.; Cao, Y. *Adv. Mater.* **2004**, *16*, 1826–1830. (b) Hoven, C. V.; Yang, R.-Q.; Garcia, A.; Crockett, V.; Heeger, A. J.; Bazan, G. C.; Nguyen, T.-Q. *Proc. Natl. Acad. Sci. U.S.A.* **2008**, *105*, 12730–12735. (c) Lin, C.-Y.; Garcia, A.; Zalar, P.; Brzezinski, J. Z.; Nguyen, T.-Q. *J. Phys. Chem. C* **2010**, *114*, 15786–15790.

(7) (a) Jiang, H.; Taraneckar, P.; Reynolds, J. R.; Schanze, K. S. *Angew. Chem., Int. Ed.* **2009**, *48*, 4300–4316. (b) Hoven, C. V.; Garcia, A.; Bazan, G. C.; Nguyen, T.-Q. *Adv. Mater.* **2008**, *20*, 3793–3810. (c) Huang, F.; Wu, H.-B.; Cao, Y. *Chem. Soc. Rev.* **2010**, *39*, 2500–2521.

(8) (a) Yang, R.-Q.; Xu, Y.-H.; Dang, X.-D.; Nguyen, T.-Q.; Cao, Y.; Bazan, G. C. *J. Am. Chem. Soc.* **2008**, *130*, 3282–3283. (b) Liu, G.; Li, A.-Y.; An, D.; Wu, H.-B.; Zhu, X.-H.; Li, Y.; Miao, X.-R.; Deng, W.-L.; Yang, W.; Cao, Y.; Roncali, J. *Macromol. Rapid Commun.* **2009**, *30*, 1484–1491. (c) Pho, T. V.; Zalar, P.; Garcia, A.; Nguyen, T.-Q.; Wudl, F. *Chem. Commun.* **2010**, *46*, 8210–8212.

(9) Hoven, C. V.; Peet, J.; Mikhailovsky, A.; Nguyen, T.-Q. *J. Appl. Phys.* **2009**, *94*, No. 033301.

(10) (a) Ho, P. K. H.; Granström, M.; Friend, R. H.; Greenham, N. C. *Adv. Mater.* **1998**, *10*, 769–774. (b) de Boer, B.; Hadipour, A.; Mandoc, M. M.; van Woudenbergh, T.; Blom, P. W. M. *Adv. Mater.* **2005**, *17*, 621–625. (c) Winroth, G.; Fenwick, O.; Scott, M. A.; Yip, D.; Howorka, S.; Cacialli, F. *Appl. Phys. Lett.* **2010**, *97*, No. 043304.

(11) (a) Seo, J. H.; Yang, R.-Q.; Brzezinski, J. Z.; Walker, B.; Bazan, G. C.; Nguyen, T.-Q. *Adv. Mater.* **2009**, *21*, 1006–1011. (b) Fang, J.-F.; Wallikewitz, B. H.; Gao, F.; Tu, G.-L.; Müller, C.; Pace, G.; Friend, R. H.; Huck, W. T. S. *J. Am. Chem. Soc.* **2011**, *133*, 683–685. (c) Li, H.-P.; Xu, Y.-H.; Hoven, C. V.; Li, C.-Z.; Seo, J. H.; Bazan, G. C. *J. Am. Chem. Soc.* **2009**, *131*, 8903–8912.

(12) (a) *Physical Chemistry of Polyelectrolytes*; Radeva, T., Ed.; Surfactant Science Series, Vol. 99; Marcel Dekker: New York, 2001. (b) Manning, G. S. *Annu. Rev. Phys. Chem.* **1972**, *23*, 117–140. (c) Dobrynin, A. V.; Rubenstein, M. *Prog. Polym. Sci.* **2005**, *30*, 1049–1118.

(13) (a) Yumusak, C.; Singh, T. B.; Sariciftci, N. S.; Grote, J. G. *Appl. Phys. Lett.* **2009**, *95*, No. 263304. (b) Sun, Q.-J.; Chang, D. W.; Dai, L.-M.; Grote, J.; Naik, R. *Appl. Phys. Lett.* **2008**, *92*, No. 251108. (c) Hagen, J. A.; Li, W.; Steckl, A. J.; Grote, J. G. *Appl. Phys. Lett.* **2006**, *88*, No. 171109. (d) Kobayashi, N.; Umemura, S.; Kusabuka, K.; Nakahira, T.; Takashi, H. *J. Mater. Chem.* **2001**, *11*, 1766–1768. (e) Koyama, T.; Kawabe, Y.; Ogata, N. *Proc. SPIE* **2002**, *4464*, 248–255. (f) Hirata, K.; Oyamada, T.; Imai, T.; Sasabe, H.; Adachi, C.; Kimura, T. *Appl. Phys. Lett.* **2004**, *85*, 1627–1629.

(14) (a) Steuerman, D. W.; Garcia, A.; Dante, M.; Yang, R.-Q.; Löfvander, J. P.; Nguyen, T.-Q. *Adv. Mater.* **2008**, *20*, 528–534. (b) Wang, C.; Garcia, A.; Yan, H. P.; Sohn, K. E.; Hexemer, A.; Nguyen, T.-Q.; Bazan, G. C.; Kramer, E. J.; Ade, H. *J. Am. Chem. Soc.* **2009**, *131*, 12538–12539.

(15) (a) Parker, I. D. *J. Appl. Phys.* **1994**, *75*, 1656–1666. (b) Vissenberg, M. C. J. M.; Blom, P. W. M. *Mater. Sci. Eng., R* **2000**, *27*, 53–94.

(16) Chen, Z.; Dang, X.-D.; Gutacker, A.; Garcia, A.; Li, H.-P.; Xu, Y.-H.; Ying, L.; Nguyen, T.-Q.; Bazan, G. C. *J. Am. Chem. Soc.* **2010**, *132*, 12160–12162.

(17) (a) Bozano, L.; Carter, S. A.; Scott, J. C.; Malliaras, G. G.; Brock, P. J. *Appl. Phys. Lett.* **1999**, *74*, 1132–1134. (b) Lin, H.-N.; Lin, H.-L.; Wang, S.-S.; Yu, L.-S.; Perng, G.-Y.; Chen, S.-A.; Chen, S.-H. *Appl. Phys. Lett.* **2002**, *81*, 2572–2574. (c) Dante, M.; Yang, C.; Walker, B.; Wudl, F.; Nguyen, T.-Q. *Adv. Mater.* **2010**, *22*, 1835–1839. (d) Reid, O. G.; Munechika, K.; Ginger, D. S. *Nano Lett.* **2008**, *8*, 1602–1609.

(18) (a) Grüner, J.; Remmers, M.; Neher, D. *Adv. Mater.* **1997**, *9*, 964–968. (b) Baigent, D. R.; Greenham, N. C.; Grüner, J.; Marks, R. N.; Friend, R. H.; Moratti, S. C.; Holmes, A. B. *Synth. Met.* **1994**, *67*, 3–10.